© IWA Publishing 2021
247

Water Practice & Technology Vol 16 No 1
doi: 10.2166/wpt.2020.110

Effect of blocked trash rack on open channel infrastructure

Mahmoud Zayed[a,*] and Elzahry Farouk[b]

[a] National Water Research Center, Channel Maintenance Research Institute, Kalubia 13621, Egypt

[b] Shoubra Faculty of Engineering, Water Resources and Hydraulics Division, Benha University, Cairo 11625, Egypt

*Corresponding author. E-mail: mahmoudzayed13@yahoo.com; mahmoud_zayed@nwrc.gov.eg

Abstract

Rack clogging can produce dramatic changes in channel hydraulics. Previous studies have investigated the hydraulics of trash racks for various parameters, but the methodology and the findings were not sufficiently refined. Free-surface depression has also been neglected so far. This study considers the rack blockages as impermeable and box-shaped accumulations (instead of considering their bar thicknesses or spacings) for the hydraulic conditions. Hence, flume experiments were performed to clarify the impact of the governing variables on the rack head loss and to examine the characteristics of free-surface depression (i.e. the length of free-surface depression and maximum depth of the depression) because of predefined blockage ratios. The results prove that the rack head loss and flow turbulence behind the rack mainly depend on the rack blockage and Froude number. However, the results for the blockage ratio $\leq$0.13 at the approach Froude number $\leq$0.12 has a minor effect on the resulting rack head loss; therefore, the effects are negligible. This study proposed design equations that determine the rack head loss, length of free-surface depression, and maximum depth of the depression behind the rack because of the box-shaped accumulation body that could be used by water engineers. Furthermore, the study improves upon the process understanding of rack blockages to avoid the potential hazards of open channel infrastructure.

Key words: blockage ratio, free surface depression, head loss, open channel, vertical trash rack

Highlights

- This study considers the rack blockages as impermeable and box-shaped accumulations for hydraulic conditions.
- Flume experiments were performed to clarify the impact of governing variables on the rack head loss.
- We propose design equations that determine the rack head loss, length of free-surface depression, and maximum depth of the depression behind the rack.
- The study improves upon the process understanding of rack blockages to avoid potential hazards of open channel infrastructure.

NOTATION

A_b	wetted area of the box-shaped plate
A_s	wetted area of the bars and supports
A_t	total wetted area of the rack field
B	blockage ratio as presented in Equation (2)
d	depth of box-plate blockage in the vertical direction
E_u	energy at upstream
F_o	approach flow Froude numbers
F_u	upstream Froude numbers in case of rack blockage
g	gravitational acceleration
h_d	downstream water depth

Water Practice & Technology Vol 16 No 1
doi: 10.2166/wpt.2020.110

h_m maximum depth of the depression
h_o approach flow depth
h_u upstream water depth
L_d length of the free-surface depression
Q flow discharge
R_o approach Reynolds number
U_o approach flow velocity
U_u upstream mean velocity
α rack angle
ΔE_{ud} energy loss
Δh hydraulic head loss
ξ head loss coefficient
υ kinematic viscosity

INTRODUCTION

One main difficulty that confronts stream crossing structures is debris. This debris can accumulate at the openings and culverts of bridge structures, producing a damaging impact on the structure's operations (Chang & Shen 1979; Diehl 1997). The trash rack is one main countermeasure that is used to trap debris and stop it from entering open structures and causing undesirable outcomes (Bradley *et al.* 2005; EA 2009). However, debris racks face a major hazard with harmful consequences caused by rack clogging (EA 2009). Trash rack blockage can block the waterway openings and increase the backwater, thereby increasing the potential for flooding and destroying nearby infrastructure.

Many researchers have investigated the accumulation and impact of debris at river structures (Stockstill *et al.* 2009; Weitbrecht & Rüther 2009; Tamagni *et al.* 2010). In their field study, Ibrahim *et al.* (2015) investigated the debris accumulation upstream of the hydroelectric power station of New Naga Hammady Barrages in the Nile River. This research aimed to investigate the impact of debris accumulation at the trash racks of hydroelectric facilities and turbines, which negatively affected electricity production. In addition, the racks were designed for specific locations to counter transported debris from high-yield source areas before reaching the hydroelectric power station or turbine racks.

The backwater rise because of large wood accumulations has been investigated by certain researchers (Rimböck 2003; Elliot *et al.* 2012; Gems *et al.* 2012; Schmocker & Hager 2013; Schmocker &Weitbrecht 2013; Ruiz-Villanueva *et al.* 2014). Schalko *et al.* (2018) conducted flume experiments with a fixed bed to detect the effect of the hydraulic conditions; they also investigated large wood accumulation characteristics on the backwater rise Δh for two model scales. The organic fine material, accumulation compactness and length, and log diameter were used to identify the effect of large wood characteristics on Δh, as follows:

$$\frac{\Delta h}{h_o} - 5.4 LW_D = 5.4 \frac{F_o I^{1/3}(9Fm + 1)}{K^{1/3}} \tag{1}$$

where h_o = approach flow depth, LW_D = dimensionless large wood accumulation factor, F_o = approach Froude number, I = flow diversion factor = ratio between length of accumulation and mean log diameter, Fm = organic fine material, hereby described as leaves and branches in an accumulation, and added as a volume percentage of the solid large wood volume V_S, and K = bulk factor = ratio between the loose large wood volume V_L and V_S. However, it is difficult to define the large wood characteristics to estimate Δh in natural cases, especially with different debris mixtures.

In most previous studies, the hydraulic conditions or head losses of racks were, for example, by using the effect of bar thickness, spacing, or blockage ratio (e.g. Kirschmer 1926; Osborn 1968; Clark *et al.* 2010; Raynal *et al.* 2013a, 2013b; Albayrak *et al.* 2018). However, examining different bar thicknesses or spacings as blockages without attaching debris does not adequately represent the natural blockage effect on the trash racks because of the differences in the blockage locations

Water Practice & Technology Vol 16 No 1
doi: 10.2166/wpt.2020.110

and distributions. Josiah *et al.* (2016) examined an inclined trash rack with circular bars; they used clear bar spacings of 5 and 10 mm and bar diameters of 2, 3, 6, 8, 10 mm to obtain different blockage ratios that varied from 0.17 to 0.68 during the study. Based on their results, they proposed the head loss equation by using all possible parameters that affected rack losses, such as the blockage ratio, unit discharge, and inclination angle with the channel bed. Böttcher *et al.* (2019) experimentally compared the trash rack with circular bars and fish protection systems (flexible fish fence made using horizontal cables instead of bars for different bar and cable spacings). The results showed that the head loss coefficient was independent of the tested Bar–Reynolds number. In addition, a design equation was proposed to estimate the head loss for both rack options. A few studies have been performed for flow through bar racks using numerical analyses (e.g. Hermann *et al.* 1998; Meusburger *et al.* 1999), as exemplified by Tsikata *et al.* (2014).

Several studies have been performed to understand the characteristics of turbulent flow around cylinders (Nakagawa *et al.* 1999; Dutta *et al.* 2003; Agelinchaab *et al.* 2008). Agelinchaab *et al.* (2009) exemplified how Knisely (1990) and Matsumoto (1999) presented excellent reviews of flows around rectangular cylinders. Agelinchaab *et al.* (2009) studied the turbulence characteristics of pairs of identical rectangular and streamlined cylinders in an open channel of varying cylinder inclinations using particle image velocimetry. They observed that a strong asymmetric flow pattern occurred when the cylinder inclination increased. In addition, the induced asymmetric hydrodynamic loads could lead to more vibration problems and eventually to structural failures.

Most studies on rack hydraulic conditions, in particular, on head loss due to blockages have focused on the bar spacing or the thickness. However, a knowledge gap exists on the hydraulic rack losses related to the blockages from debris clogging; these blockages have been simplified into a horizontal box shape in this study. Furthermore, to the best of our knowledge, no former study has addressed detailed descriptions about the characteristics of free-surface depression using designing equations because of predefined horizontal blockages. Therefore, this experimental study is aimed at clarifying the effects of various rack blockages arising from debris on the head loss and the length and maximum depth of the free-surface depression downstream of the rack for a vertical trash rack with a fixed bed.

EXPERIMENTAL SETUP

The flume experiments were conducted in a trapezoidal open channel at the Hydraulic Laboratory of Channel Maintenance Research Institute, National Water Research Center, Egypt. The channel was 16.22 m long, 0.42 m deep, and 0.6 m wide. The experimental equipment has been described in greater detail in Zayed *et al.* (2018a, 2018b).

To study the rack hydraulic behaviors, a rack was placed vertically and perpendicular to the channel within a fixed bed 8 m downstream of the intake. The rack always consists of vertical mild steel bars that are circular; they are 3 mm in diameter, 25 cm deep, and have a clear spacing of 20 mm. The welded rack bars were supported by outer bars and fixed to the flume side wall. The outer supporting structure was minimized, and consequently the rack itself (bars and outer supports) had hardly any influence on the head loss and approach flow conditions.

The rack blockage was modeled and mounted on the trash rack at the water-level height as a plate in the shape of an impermeable box. Actually, the wetted rack components (bars and outer supports) represented the blockage ratio of $B = 0.08$ (Figure 1). Instead of changing the bar diameter and spacing, plates of various sizes with depths of $d = 2.3$, 2.9, 3.6, 6.0, 7.5, 9.6, and 12.0 cm in the vertical direction were attached to the rack to obtain the blockage ratios of $B = 0.13$, 0.25, 0.32, 0.45, 0.50, 0.64, and 0.69, respectively. In fact, the predefined debris plate blockage (impermeable and regular shape) was comparable with the debris blockage proposed by Melville & Dongol (1992). The rack blockage simulation study concerns the rack accumulation caused by the floating debris. Because

Water Practice & Technology Vol 16 No 1
doi: 10.2166/wpt.2020.110

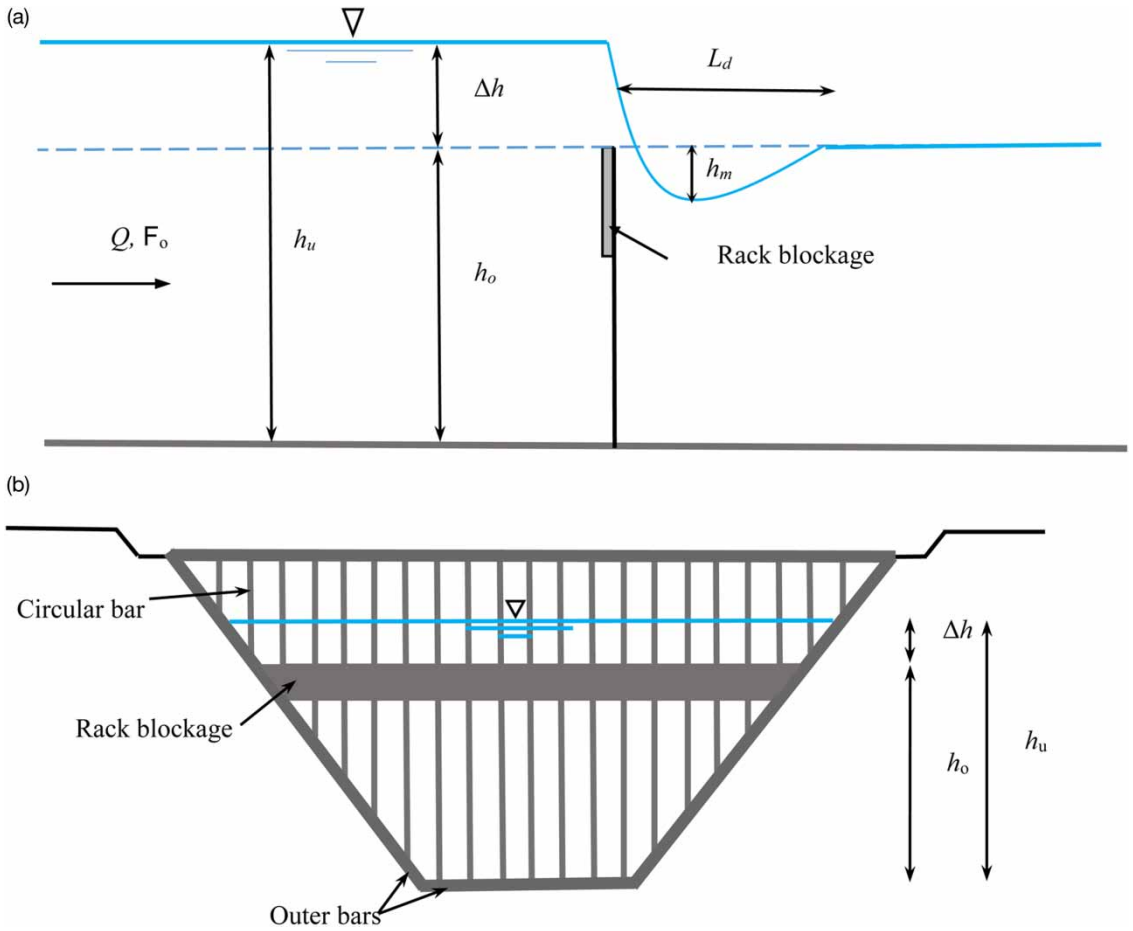

Figure 1 | Rack model in the channel (a) side view and (b) upstream view.

of the additional accumulation, the debris is dragged to the bottom of the rack, and the accumulation is extended vertically downward (see Schmocker & Hager 2013; Schalko *et al.* 2019a, 2019b). Furthermore, Hartlieb (2015) illustrated that the accumulation body was considerably less permeable because of the additional organic fine material (e.g. leaves and small branches). Actually, the initial debris accumulation has a major effect on the backwater rise; the debris properties and the mixture have a negligible effect (Schmocker & Hager 2013). From the field observation experiences, the different accumulation layers at the back of the initially trapped rack accumulations can create an impermeable accumulating body. Accordingly, the proposed debris blockage can efficiently simulate natural observations. The blockage ratio B is calculated using the following expression:

$$B = \frac{A_b + A_s}{A_t}, \tag{2}$$

where A_b is the wetted area of the box-shaped plate; A_s is the wetted area of the bars and supports; and A_t is the total wetted area of the rack field.

In all the experiments and flow rates, the approach flow depth of $h_o = 25$ cm was maintained by the predefined tail gate openings. Given the approach flow conditions (subscript o) measured without the rack blockage, a defined flow discharge $Q = 20$, 25, 30, 35, and 40 L/s resulted in the approach flow Froude numbers $F_o = (U_o/[gh_o]^{0.5}) \approx 0.06$, 0.07, 0.08, 0.01, and 0.12, respectively; these numbers were based on the approach flow velocity U_o, approach flow depth h_o, and gravitational acceleration g. The corresponding Reynolds number ($R_o = U_o h_o/\upsilon$) varied from 21625 to 46088 based on the approach flow velocity, flow depth, and kinematic viscosity υ. Therefore, all the experiments were performed

Water Practice & Technology Vol 16 No 1
doi: 10.2166/wpt.2020.110

Table 1 | Parameter range and test conditions

Parameters	Range
Q	20–40 L/s
B	0.08–0.69
F_o	0.06–0.12
R_o	21,625–46,088
h_o	25 cm
$U_u^2/2g$	0.05–0.14 cm

with the turbulent and subcritical approach flow regimes. The Reynolds number based on the approach flow velocity and rack blockage depth ($R_d = U_o d/\upsilon$) varied from 2165 to 22588 (Table 1). To identify the water surface elevations for the rack with different configurations, the upstream and downstream water surfaces were measured by a point gauge at mid span along the channel at x intervals of 10 cm. However, because of the disturbed flow, the measurements of the downstream water surface were taken at several locations to obtain the average value. The characteristics of free-surface depression were detected from these data. To calculate the hydraulic head loss Δh, the upstream and downstream water depths (h_u and h_d, respectively) were measured carefully at $x = -1.5$ m and at $x =$ 4.5 m, respectively to avoid the turbulence zone; we took $x = 0$ m at the rack foot. The head loss coefficient ξ is determined as follows:

$$\Delta h = \xi \frac{U_u^2}{2g} \tag{3}$$

where U_u is the upstream mean velocity, and g is the gravitational acceleration.

OBSERVATIONS AND RESULTS

Rack head loss

The effect of F_o and B on ξ was examined in the range of $F_o = 0.06$–0.12 and $B = 0.08$, 0.13, 0.25, 0.32, 0.45, 0.50, 0.64, and 0.69. In Figure 2, ξ is plotted as a function of B for various F_o. As shown by Zayed

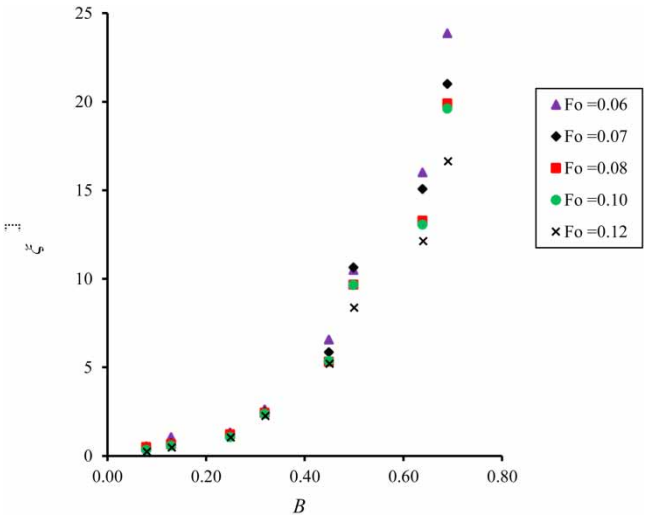

Figure 2 | Head loss coefficient ξ versus blockage ratio B for various F_o.

Water Practice & Technology Vol 16 No 1
doi: 10.2166/wpt.2020.110

et al. (2018a, 2018b, 2020), the head loss coefficient increases strongly with B. This is because the increasing blockage ratio decreases the rack surface area, which results in an increased ξ value. Regarding the blockage ratio effect, the rack with $B = 0.25$, 0.32, 0.45, 0.50, 0.64, and 0.69 increases ξ by approximately 1.6, 5, 12, 20, 31, and 45.5 times, respectively, as compared with the rack with $B = 0.08$ (Figure 2). This means that the blockage ratios significantly affect the rack head loss coefficients and should not be larger than 25% for additional safety. In addition, large uncertainties are observed for $F_o < 0.12$, which correspond to the measurements of $B < 0.32$ based on the head loss coefficients, in which the head losses are so low that they cannot be accurately measured; this results in high relative uncertainties. It further proves that the development of head loss as a function of the blockage ratio is not linear.

The effect of the approach Froude number on Δh was investigated for various B values. Figure 3 shows Δh as a function of F_o in the range of $B = 0.08$–0.69. The head loss increases with F_o for each blockage ratio. Moreover, Δh appears clearly with the blockage ratio (Figure 3). For $F_o = 0.12$, Δh resulted in 0.39 cm for $B = 0.32$ as compared with $\Delta h = 1.45$ cm for $B = 0.50$. This is because a higher blockage ratio represents a greater flow resistance, which leads to greater head loss. For $F_o < 0.12$ with $B < 0.13$, the Δh values can be neglected; this is because of low velocity with low flow resistance, which reduces the drag force. Figure 4 shows the relationship between the upstream Froude number in the case of blockage ratio and approach Froude number. For a lower B ($B < 0.13$),

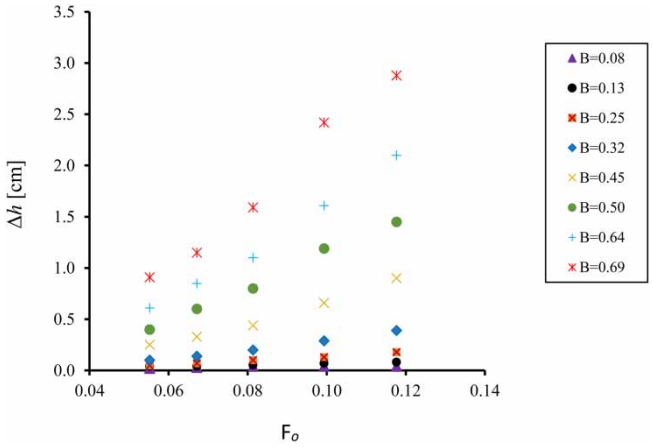

Figure 3 | Head loss Δh versus approach Froude number F_o for various B.

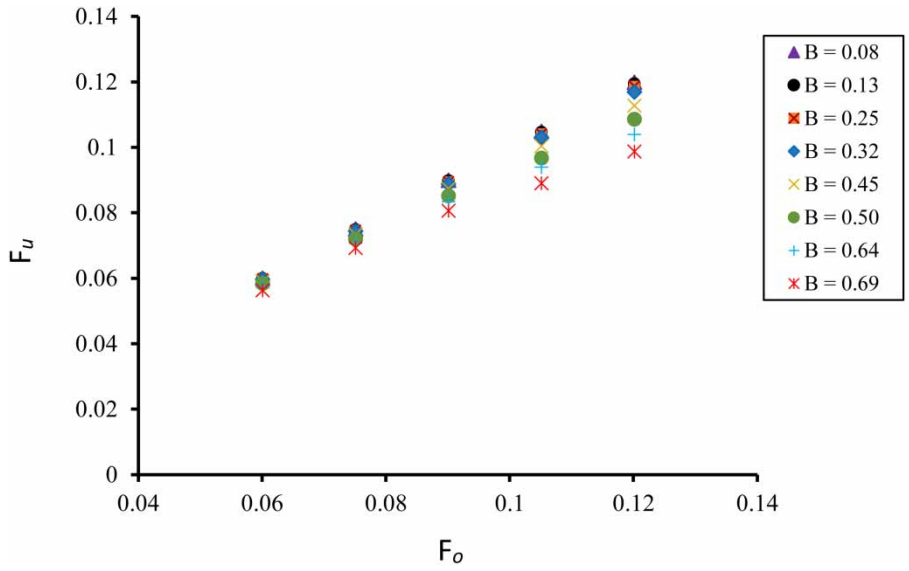

Figure 4 | Upstream Froude number F_u versus approach Froude number F_o for different blockage ratios.

Water Practice & Technology Vol 16 No 1
doi: 10.2166/wpt.2020.110

the curve shows that the impact of F_o on F_u is not significant in the range of $F_o < 0.12$ because of low backwater rise. In general, the F_u values decrease with increasing B based on the results. For $F_o = 0.12$, F_u resulted in 0.118 for $B = 0.25$ compared with $F_u = 0.098$ for $B = 0.69$. Due to the higher blockage ratio, the upstream backwater rise increases, which results in a lower F_u. Actually, the introduction of F_u simplifies the rack loss assessment in the field measurements because F_o is associated with uncertainties resulting from unexpected blockage ratios. Therefore, the upstream Froude number due to the blockage can be described by a relationship with the approach Froude number $F_o = 0.06$–0.12 ($R^2 = 0.95$).

$$F_u = 0.94F_o \tag{4}$$

Design equation for rack head loss

An attempt was made to estimate the rack head loss, and the regression model was applied to the proposed Equation (5) using the experimental data. Based on F_o, F_u can be defined as Equation (4) for practical applications.

$$\xi = 8.13B^{1.84}F_o^{-0.49} \tag{5}$$

Clearly, Equation (5) has been developed for the classical screen (perpendicular and vertical to the flow direction) with box-shaped plates, which is a concept different from the bar diameters and spacings. In particular, the proposed equation is valid for $0.06 \leq F_o \leq 0.12$, $0.08 \leq B \leq 0.69$ and circular bars. As presented in Equation (5), the largest effective factor on ξ is the blockage ratio with an exponent of 1.84. The fit of Equation (5) has a high adjusted R^2 value of 0.93, which indicates a good fit to the experimental data. Moreover, the standard errors of the independent coefficients are 0.07 and 0.21, whereas the highest value represents the approach Froude number F_o and the lowest value the blockage ratio. Actually, the high standard error for F_o is due to the low velocity, which results in a low drag force; therefore, the uncertainties for F_o increase in the experimental tests. Figure 5 shows a comparison between the measured and predicted head loss by Equation (5). In Figure 5, the coefficient of determination R^2 and the standard error are 0.95 and 0.13, respectively. Figure 5 shows that the uncertainty zone or overestimation of Δh (highlighted in red) for the measured $\Delta h < 0.5$ cm. These points refer to Δh recorded at $B < 0.25$ for $F_o < 0.12$. Actually, this zone is consistent with the results in Figures 2 and 3 because of the low drag force (as discussed previously). Besides the

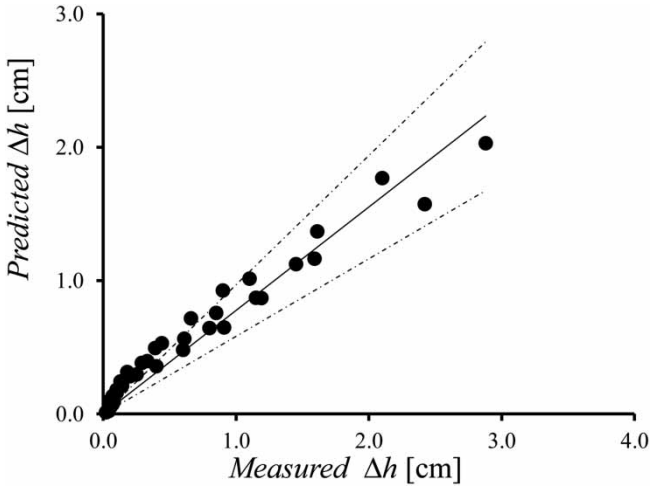

Figure 5 | Comparison between the measured head loss and the predicted by Equation (5), and ±25% prediction range.

Water Practice & Technology Vol 16 No 1
doi: 10.2166/wpt.2020.110

uncertainty zone, 88% of the data falls within the 25% predicted range, which implies that the results are within the acceptable band. Therefore, it is recommended to apply Equation (5) for $\Delta h > 0.5$ cm.

Characteristics of free-surface depression

The investigations of (1) length of the free-surface depression L_d and (2) maximum depth of the depression h_m downstream of the rack were analyzed for various blockage ratios and approach Froude numbers.

Figure 6 depicts the depression (dip) in the free-surface through the vertical rack ($\alpha = 90°$, $F_o = 0.06$–0.12, $B = 0.08$–0.69) at selected streamwise locations x/h_o between -4.8 and $+15.4$. The upstream flow of the rack is generally streamwise, but it is not exactly uniform. Actually, slight bends occur upward near the rack because of the flow deceleration caused by the rack obstruction. Figure 6 shows the variations in depression (dip) in the free surface immediately behind the rack for different blockage ratios and reference values (no rack). The presence of the rack substantially creates flow disturbances behind the rack because of the associated flow contraction, and the degree of this disturbance or free-surface depression depends on both the blockage ratios and approach Froude numbers. As the blockage ratio and Froude number increase, the downstream flow is severely disturbed, and the depression increases as well (Figure 7 and Table 2). Then, in a region far downstream the rack, the flow converts into a uniform condition. Regarding the bed stability and level measurements, it is recommended to consider the depression characteristics in the construction processes.

Length of free-surface depression

The effect of F_o and B on the relative length of the free-surface depression L_d/h_u was examined in the tested range conditions. In Figure 8, L_d/h_u was plotted as the function F_o for various B values. For $B = 0.69$, L_d/h_u was 5.21 for $F_o = 0.06$ as compared with 13.8 for $F_o = 0.12$. Obviously, for the same blockage ratio, L_d/h_u increases with increasing F_o, and it becomes stronger for higher blockage ratios. This fact results from the increase of the approach flow velocity with increasing F_o and a corresponding increase in the vibration amplitudes. Besides the Froude number, L_d/h_u is also affected by B; L_d/h_u increases with the increasing blockage ratio. For $F_o = 0.12$, L_d/h_u resulted in 10.77 for $B = 0.50$ as compared with $L_d/h_u = 12.36$ for $B = 0.64$. In particular, a high blockage ratio induced a high flow disturbance, which increased the L_d/h_u value for each F_o (see Naudascher & Rockwell 2012; Tsikata *et al.* 2014; Böttcher *et al.* 2019). In other words, for a certain rack configuration, the free-surface depressions extend over a longer distance as the blockage ratio and Froude number increase (see Tsikata *et al.* 2009). Note that the flow disturbance induces an undesirable outcome for the rack circular bars and turbine components because of the flow vibration, thereby increasing their stiffness, which should be considered in the optimization processes (Figure 9). To simplify the findings, Equation (6) reflects the relationship between the relative length of the depression, its independent parameters blockage ratio, and the approach Froude number, which can be replaced by the upstream Froude number, as shown in Equation (4).

$$L_d/h_u = 2951.2\, B^{1.87} F_o^{2.05} \tag{6}$$

For a given blockage ratio, the resulting length of the free-surface depression [see Equation (6)] can be estimated for various approach flow conditions. This equation reveals that both the governing parameters have an exponential value of 1.87 for B, which is quite close to 2.05 for F_o at 95% probability limit; this shows that there is a significant impact on L_d/h_u. The adjusted coefficient of determination of the best fit is $R^2 = 0.95$, and the standard error is 0.14. Particularly, the standard errors of the

Water Practice & Technology Vol 16 No 1
doi: 10.2166/wpt.2020.110

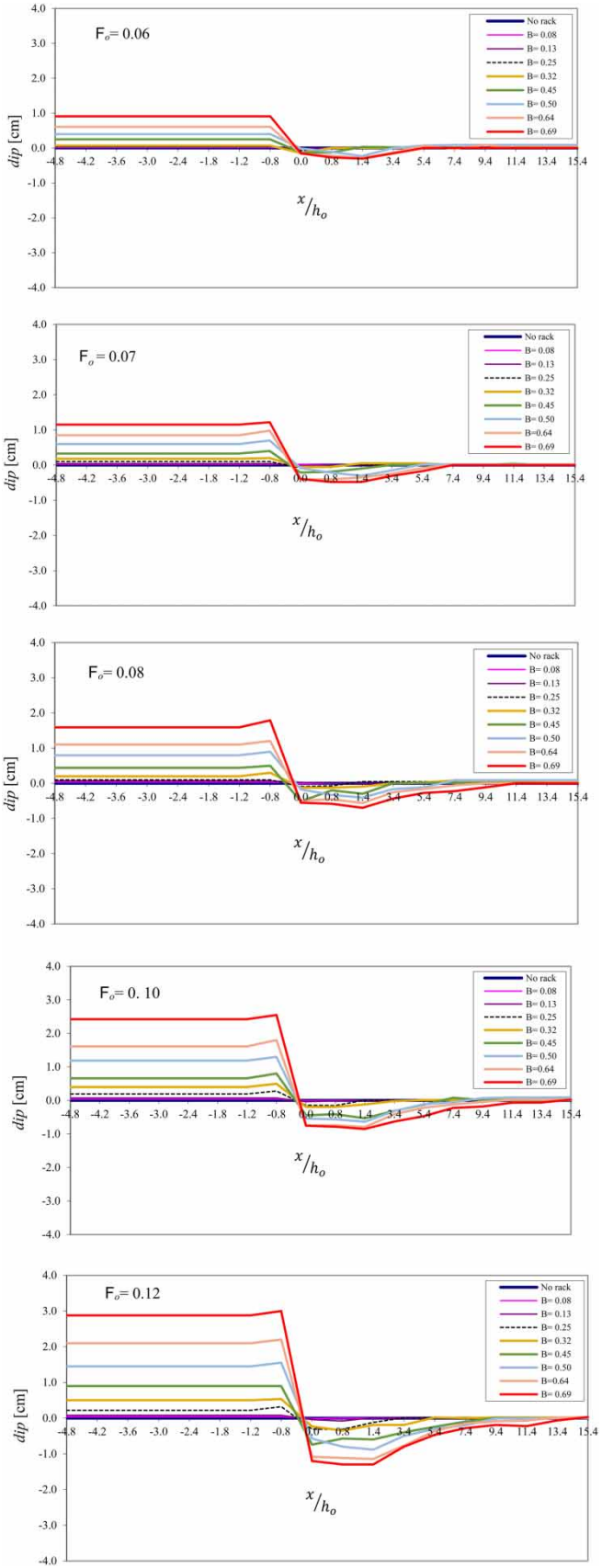

Figure 6 | Variation of dip for the different blockage ratios at approach Froude number of $F_o = 0.06$, 0.07, 0.08, 0.10, and 0.12.

Water Practice & Technology Vol 16 No 1
doi: 10.2166/wpt.2020.110

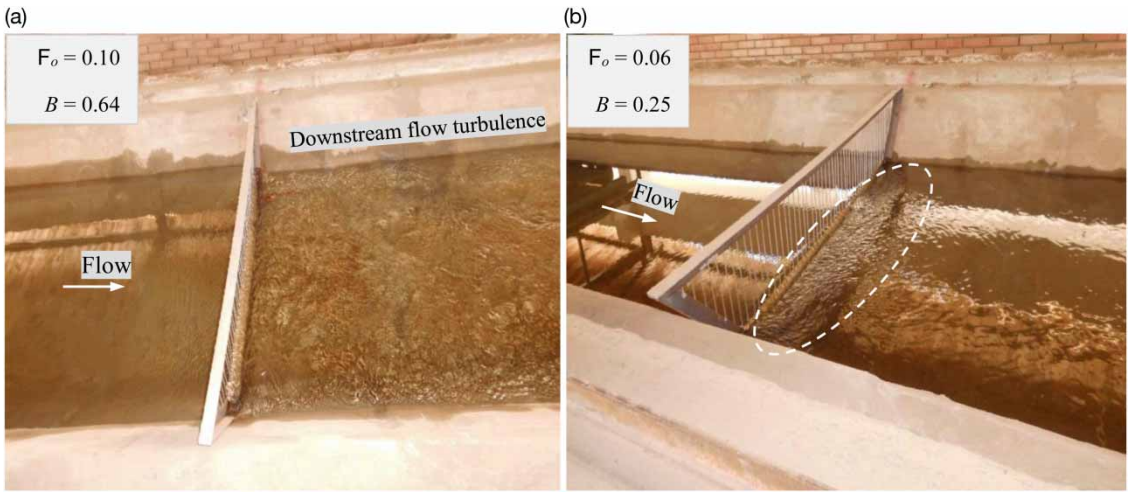

Figure 7 | Flow turbulence for (a) B = 0.64 at $F_o = 0.10$, and (b) B = 0.25 at $F_o = 0.06$.

Table 2 | Sample of experimental results

Blockage ratio	F_o	h_m (cm)	L_d (cm)
0.08	0.06	0.01	2
0.08	0.12	0.02	10
0.13	0.06	0.05	10
0.13	0.12	0.15	35
0.25	0.06	0.07	10
0.25	0.12	0.31	85
0.32	0.06	0.1	18
0.32	0.12	0.35	140
0.45	0.06	0.12	30
0.45	0.12	0.78	235
0.5	0.06	0.23	85
0.5	0.12	0.88	285
0.64	0.06	0.28	100
0.64	0.12	1.14	335
0.69	0.06	0.3	135
0.69	0.12	1.3	385

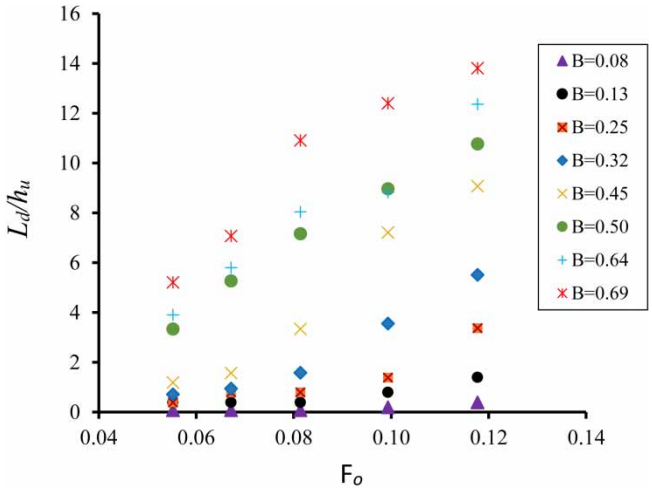

Figure 8 | L_d/h_u versus F_o for various blockage ratios.

Water Practice & Technology Vol 16 No 1
doi: 10.2166/wpt.2020.110

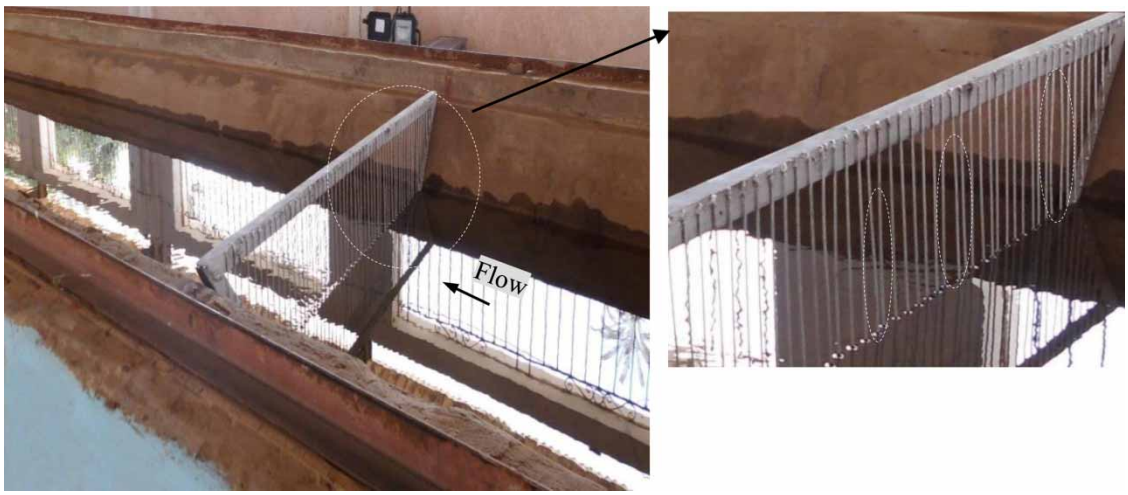

Figure 9 | Bar distortions resulting from flow disturbance and vibration.

governing parameter coefficients are 0.075 and 0.2; the highest value represents F_o, and the lowest value represents B. The measured relative length of the free-surface depression L_d/h_u is plotted against the relative predicted length of the free-surface depression using Equation (6) and $\pm 30\%$ prediction range in Figure 10. A majority of the data points fall within $\pm 30\%$; therefore, Equation (6) can be applied to estimate the length of the free-surface depression downstream of a vertical rack due to blockage. Based on Equation (6), as B increases from 0.08 to 0.25 and 0.32, the equation yields an increase of approximately 7.4 and 12.4 times in L_d/h_u, respectively, for the average F_o.

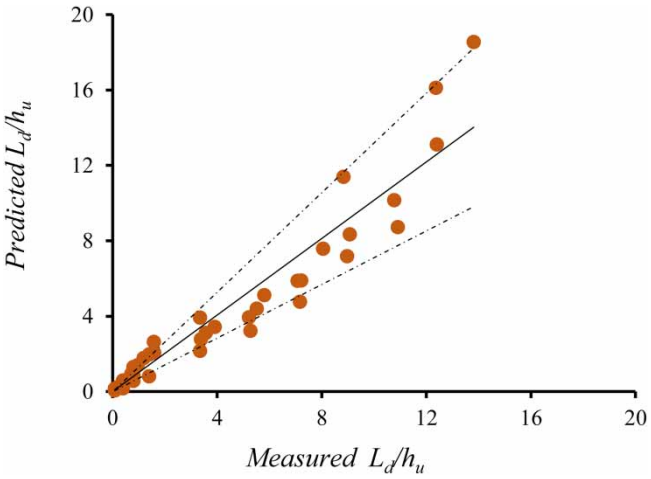

Figure 10 | Comparison between the measured L_d/h_u and the predicted by Equation (6), and $\pm 30\%$ prediction range.

Maximum depth of the depression

The relative maximum depth of the depression h_m/h_u was investigated for various F_o and B values. Figure 11 shows h_m/h_u versus the approach Froude number for different blockage ratios. Actually, h_m/h_u values for $B \leq 0.08$ at $F_o \leq 0.12$ can be neglected. The gap between the data for $F_o = 0.06$ is less than that for $F_o = 0.12$ within the range of B values, which means that the effect of the maximum depth of the depression appears gradually with F_o (Figure 11). For $B = 0.69$, h_m/h_u resulted in 0.011 for $F_o = 0.06$ compared with $h_m/h_u = 0.046$ for $F_o = 0.12$. Concerning the blockage impact, increasing

Water Practice & Technology Vol 16 No 1
doi: 10.2166/wpt.2020.110

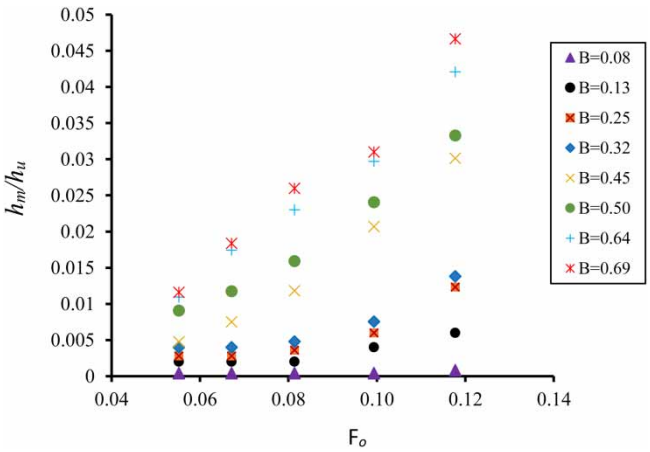

Figure 11 | h_m/h_u versus F_o for various blockage ratios.

B usually results in increasing the rack resistance and the relative maximum depth of depression, especially when considering $B > 0.08$ in the tested range of flow conditions. For $F_o = 0.12$, h_m/h_u resulted in 0.033 for $B = 0.50$ compared with $h_m/h_u = 0.042$ for $B = 0.64$. Again, these results arise from the flow disturbances at a high flow velocity with rack resistance. For both independent parameters, the maximum depth of depression increases with increasing F_o, and it evidently becomes stronger as the blockage increases, which reveals the profound impact of B and F_o on h_m/h_u. The relationship between the dimensionless term h_m/h_u and $0.06 \leq F_o \leq 0.12$ and $0.08 \leq B \leq 0.69$ based on the regression analysis is as follows:

$$h_m/h_u = 3.23\, B^{1.68}\, F_o^{1.68} \tag{7}$$

From Equation (7), both B and F_o have an exponent value of 1.68 at 95% probability limit, which reveals significant predictive factors. The standard error of Equation (7) is 0.14, and the adjusted coefficient of determination of the best fit is $R^2 = 0.94$, which signifies a reliable fit of the experimental data. The standard errors of the B and F_o coefficients are 0.07 and 0.2, respectively, whereas the highest value represents F_o, and the lowest value represents B. Figure 12 shows the measured relative maximum depth of the depression h_m/h_u versus the relative predicted maximum depth of the depression using Equation (7) and $\pm 20\%$ prediction range. Actually, a majority of the data points are clustered in the prediction range, which presents a good fit to Equation (7) for describing the

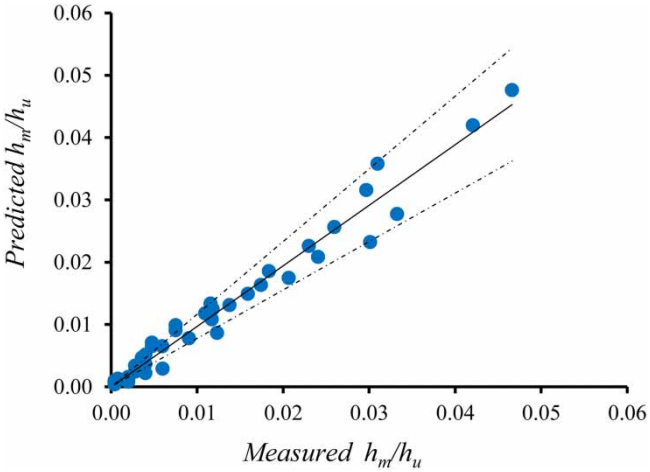

Figure 12 | Comparison between the measured h_m/h_u and that predicted by Equation (7), and $\pm 20\%$ prediction range.

Water Practice & Technology Vol 16 No 1
doi: 10.2166/wpt.2020.110

maximum depth of the depression for various blockages. For the average F_o, B increases from 0.08 to 0.25, whereas Equation (7) yields an increase of approximately 5.6 times in h_m/h_u. A further increase to $B = 0.32$, increases h_m/h_u by 9.2 times.

Relative energy loss

In a subcritical flow regime, the energy loss through the rack was investigated to scrutinize the impact of rack operations for various blockage ratios on the flow behavior. During the experiments, the energy loss (ΔE_{ud}) between the upstream and downstream ends of the vertical rack was obtained at $x = -1.5$ m and at $x = 4.5$ m, respectively ($x = 0$ m at the rack foot). The relative energy loss with regard to the upstream end ($\Delta E_{ud}/E_u$) is calculated using the following expression:

$$\frac{\Delta E_{ud}}{E_u} = \frac{\left(h_u + \frac{U_u^2}{2g}\right) - h_d + \frac{U_d^2}{2g}}{\left(h_u + \frac{U_u^2}{2g}\right)} \times 100 \tag{8}$$

where h_u and h_d are the flow depths at the upstream and downstream ends of the rack, respectively. Also, U_u and U_d represent the average flow velocities at the upstream and downstream ends of the the rack, respectively; these velocities are obtained by dividing the flow discharge by the cross-sectional area. In Figure 13, $\Delta E_{ud}/E_u$ is plotted as a function of F_u for different $B = 0.08$–0.69. Figure 13 shows that by increasing the subcritical F_u, the relative energy loss increases. The relative energy loss $\Delta E_{ud}/E_u$ for $B = 0.50$ increases from $\Delta E_{ud}/E_u = 1.56\%$ for $F_u \approx 0.06$ to $\Delta E_{ud}/E_u = 5.36\%$ for $F_u \approx 0.11$. In addition, a large B value represents a high flow turbulence and resistance, which results in a high loss of relative energy. For $F_u \approx 0.11$, $\Delta E_{ud}/E_u = 1.5\%$ for $B = 0.32$, whereas $\Delta E_{ud}/E_u = 3.39\%$ for $B = 0.45$.

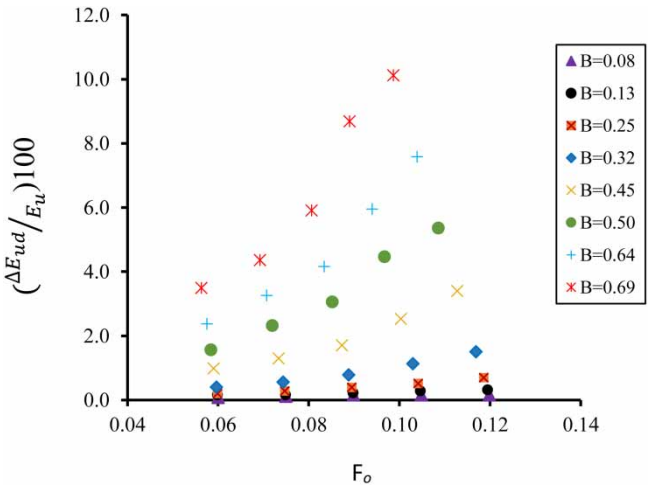

Figure 13 | Relative energy loss $\Delta E_{ud}/E_u$ versus F_u for various blockage ratios.

Comparison with previous studies

A majority of the previous reviews dealt with the rack blockage by changing the bar spacing or thickness and deduced the head loss equations based on this concept (Kirschmer 1926; Raynal *et al.* 2013a; Josiah *et al.* 2016). However, this concept did not consider three main critical issues. First, the independent variable in natural observation is the accumulated body of debris, which

Water Practice & Technology Vol 16 No 1
doi: 10.2166/wpt.2020.110

continuously changed over time at the bars rack; whereas, the bars spacing or thickness remained constant. Second, the location of the blockage can affect the rack backwater rise (Abt *et al.* 1992); therefore, the distribution of blockage using bar spacing or thickness differs from the natural blockage observations. Third, from practical application, the rack designer designs the bar rack for a minimum bar blockage to obtain negligible head loss; therefore, the bar shape (except for stiffness and fish-friendliness racks that require narrow bar spacing) will have limited benefits on the rack loss. The bar shape effect appears with the bar blockage ratio for bar configurations in the flow direction. In other words, the design of the high bar blockage is not useful for practical applications because the natural blockage arises from the accumulated body of debris. Hence, this study focused on the blockage resulting from the accumulation of debris at the bar racks for the different configurations to simulate natural performances.

Previous studies on backwater rise arising from large wood accumulations (Schalko *et al.* 2019a, 2019b) concentrated on the accumulation of volume characteristics (accumulation length, large wood diameter, compactness, and the organic fine material) at the racks. The introduction of clogging as an area of the accumulation body in this study simplifies the assessment of the blockage ratio because the evaluation of the effective debris volume or characteristics is associated with high uncertainties and estimation difficulties.

CONCLUSIONS

The experiments investigated the rack head loss and the characteristics of free-surface depression behind a vertical rack because of blockage by debris clogging; a horizontal box-shaped accumulation body was used. The experiments were conducted with varying blockage ratios and different approach flow conditions. The results can be summarized as follows:

- The main governing parameters to estimate ξ and the flow turbulence are B and F_o. As ξ increases with B and F_o, the relationship between ξ and B is not linear. The head loss coefficient ξ increases approximately 1.6, 5, 12, 20, 31, and 45.5 times at $B = 0.25$, 0.32, 0.45, 0.50, 0.64, and 0.69, respectively, compared with the rack with $B = 0.08$. However, at the examined range of $B \leq 0.13$ at $F_o \leq 0.12$, the rack head loss can be neglected because of the low rack blockage. Therefore, it is recommended to keep the rack with $B < 25\%$ at the range of $F_o < 0.12$ for additional safety.
- A design equation was deduced to estimate ξ [Equation (5)], and the application of this equation is recommended for a rack with horizontal box-shaped blockage as the clogging debris for $\Delta h >$ 0.5 cm.
- The degree of flow disturbance behind the rack depends on both B and F_o. When the flow is severely disturbed, and the depression increases with increasing B and F_o. This may lead to vibration problems and consequently rack failures; therefore, increasing the rack stiffness should be considered in the design process.
- Based on the dimensionless terms, the design Equations (6,7) were deduced to estimate the length L_d and the maximum depth of the depression h_m downstream of the rack for the examined range of B and F_o; this simplified the practical applications.

ACKNOWLEDGEMENTS

This study was carried out at the Hydraulics Laboratory of Channel Maintenance Research Institute (CMRI), National Water Research Center. The authors would like to acknowledge CMRI for the technical support and cooperation.

Water Practice & Technology Vol 16 No 1
doi: 10.2166/wpt.2020.110

DATA AVAILABILITY STATEMENT

All relevant data are included in the paper or its Supplementary Information.

REFERENCES

Abt, S. R., Brisbane, T. E., Frick, D. M. & McKnight, C. A. 1992 Trash rack blockage in supercritical flow. *Journal of Hydraulic Engineering* **118**(12), 1692–1696.

Agelinchaab, M., Tsikata, J. M., Tachie, M. F. & Adane, K. K. 2008 Turbulent wake of rectangular cylinder near plane wall and free surface. *AIAA Journal* **46**(1), 104–117.

Agelinchaab, M., Tsikata, J. M., Tachie, M. F. & Katopodis, C. 2009 Open channel flow over pairs of rectangular and streamlined cylinders at incidence. *Fluids Engineering Division Summer Meeting* **43727**, 1409–1417.

Albayrak, I., Kriewitz, C. R., Hager, W. H. & Boes, R. M. 2018 An experimental investigation on louvres and angled bar racks. *Journal of Hydraulic Research* **56**(1), 59–75.

Böttcher, H., Gabl, R. & Aufleger, M. 2019 Experimental hydraulic investigation of angled fish protection systems – comparison of circular bars and cables. *Water* **11**(5), 1056.

Bradley, J. B., Richards, D. L. & Bahner, C. D. 2005 *Debris Control Structures-Evaluation and Countermeasures: Hydraulic Engineering Circular 9*. Report FHWA-IF-04-016. Federal Highway Administration, Washington, USA.

Chang, F. F. & Shen, H. W. 1979 *Debris Problems in the River Environment*. Report FHWA-RD-79-62. Federal Highway Administration, Washington, USA.

Clark, S. P., Tsikata, J. M. & Haresign, M. 2010 Experimental study of energy loss through submerged trashracks. *Journal of Hydraulic Research* **48**(1), 113–118.

Diehl, T. H. 1997 *Potential Drift Accumulation at Bridges*. US Department of Transportation, Federal Highway Administration, Research and Development, Turner-Fairbank Highway Research Center.

Dutta, S., Muralidhar, K. & Panigrahi, P. 2003 Influence of the orientation of a square cylinder on the wake properties. *Experiments in Fluids* **34**(1), 16–23.

EA (Environment Agency) 2009 *Trash and Security Screen Guide*. Environment Agency, Bristol, UK.

Elliot, R. C., Froehlich, D. C. & MacArthur, R. C. 2012 Calculating the potential effects of large woody debris accumulations on backwater, scour, and hydrodynamic loads. In: *World Environmental and Water Resources Congress 2012: Crossing Boundaries*. Albuquerque, NM. American Society of Civil Engineers, Reston, VA, pp. 1213–1222.

Gems, B., Sendlhofer, A., Achleitner, S., Huttenlau, M. & Aufleger, M. 2012 Evaluierung verklausungsinduzierter Überflutungsflächen durch Kopplung eines physikalischen und numerischen Modells (Evaluation of floodplain areas due to large wood accumulation using hybrid modeling). In German. In: *Proceedings of the 12th Congress Interpraevent*. pp. 131–142.

Hartlieb, A. 2015 *Schwemmholz in Fließgewässern –Gefahren und Lösungsmöglichkeiten (Large Wood in Rivers – Hazards and Possible Solutions)*. (In German). Report 133. Chair of Hydraulic and Water Resources Engineering, TU Munich, München, Germany.

Hermann, F., Billeter, P. & Hollenstein, R. 1998 Investigations on the flow through a trashrack under different inflow conditions. *Hydroinformatics* 121–128. Balkema, Rotterdam.

Ibrahim, H., Osman, E. A., El-Samman, T. A. & Zayed, M. 2015 Aquatic weed management upstream new Naga Hammady barrages. In *Proceedings of the 18th International Water Technology Conference*. IWTC18, Sharm El-Sheikh, Egypt.

Josiah, N. R., Tissera, H. P. S. & Pathirana, K. P. P. 2016 An experimental investigation of head loss through trash racks in conveyance systems. *Engineer* **49**(1), 1–8.

Kirschmer, O. 1926 *Untersuchungen über den Gefällsverlust an Rechen*. Mitteilungen des hydraulischen Instituts der TH München, Munich, Germany.

Knisely, C. W. 1990 Strouhal numbers of rectangular cylinders at incidence: a review and new data. *Journal of Fluids and Structures* **4**(4), 371–393.

Matsumoto, M. 1999 Vortex shedding of bluff bodies: a review. *Journal of Fluids and Structures* **13**(7–8), 791–811.

Melville, B. W. & Dongol, D. M. 1992 Bridge pier scour with debris accumulation. *Journal of Hydraulic Engineering* **118**(9), 1306–1310. https://doi.org/10.1061/(ASCE)0733-9429(1992)118:9(1306).

Meusburger, H., Hermann, F. & Hollenstein, R. 1999 Comparison of numerical and experimental investigations of trashrack losses. In: *Proceedings of the 28th IAHR Congress*, Graz, Austria (CD-Rom), pp. 804–809.

Nakagawa, S., Nitta, K. & Senda, M. 1999 An experimental study on unsteady turbulent near wake of a rectangular cylinder in channel flow. *Experiments in Fluids* **27**(3), 284–294.

Naudascher, E. & Rockwell, D. 2012 *Flow-induced Vibrations: An Engineering Guide*. Courier Corporation, North Chelmsford, MA, USA.

Orsborn, J. F. 1968 Rectangular-bar trashrack and baffle headlosses. *Journal of the Power Division* **94**(2), 111–123.

Raynal, S., Courret, D., Chatellier, L., Larinier, M. & David, L. 2013a An experimental study on fish-friendly trashracks–Part 1. Inclined trashracks. *Journal of Hydraulic Research* **51**(1), 56–66.

Water Practice & Technology Vol 16 No 1
doi: 10.2166/wpt.2020.110

Raynal, S., Chatellier, L., Courret, D., Larinier, M. & David, L. 2013b An experimental study on fish-friendly trashracks–Part 2. angled trashracks. *Journal of Hydraulic Research* **51**(1), 67–75.

Rimböck, A. 2003 *Schwemmholzrückhalt in Wildbächen (Large Wood Retention in Mountain Torrents)*. (In German). Report 94. Chair of Hydraulic and Water Resources Engineering, TU Munich, München, Germany.

Ruiz-Villanueva, V., Bladé Castellet, E., Díez-Herrero, A., Bodoque, J. M. & Sánchez-Juny, M. 2014 Two-dimensional modelling of large wood transport during flash floods. *Earth Surface Processes and Landforms* **39**(4), 438–449. https://doi.org/10.1002/esp.3456.

Schalko, I., Schmocker, L., Weitbrecht, V. & Boes, R. M. 2018 Backwater rise due to large wood accumulations. *Journal of Hydraulic Engineering* **144**(9), 04018056. https://doi.org/10.1061/(ASCE)HY.1943-7900.0001501.

Schalko, I., Lageder, C., Schmocker, L., Weitbrecht, V. & Boes, R. M. 2019a Laboratory flume experiments on the formation of spanwise large wood accumulations: i. Effect on backwater rise. *Water Resources Research* **55**(6), 4854–4870. https://doi.org/10.1029/2018WR024649.

Schalko, I., Lageder, C., Schmocker, L., Weitbrecht, V. & Boes, R. M. 2019b Laboratory flume experiments on the formation of spanwise large wood accumulations: part II – effect on local scour. *Water Resources Research* **55**(6), 4871–4885. https://doi.org/10.1029/2019WR024789.

Schmocker, L. & Hager, W. H. 2013 Scale modeling of wooden debris accumulation at a debris rack. *Journal of Hydraulic Engineering* **139**(8), 827–836. https://doi.org/10.1061/(ASCE)HY.1943-7900.0000714.

Schmocker, L. & Weitbrecht, V. 2013 Driftwood: risk analysis and engineering measures. *Journal of Hydraulic Engineering* **139**(7), 683–695. https://doi.org/10.1061/(ASCE)HY.1943-7900.0000728.

Stockstill, R. L., Daly, S. F. & Hopkins, M. A. 2009 Modeling floating objects at river structures. *Journal of Hydraulic Engineering* **135**(5), 403–414.

Tamagni, S., Weitbrecht, V., Müller, U., Hunziker, R., Wyss, H., Kolb, R. & Baumann, W. 2010 Schwemmholzrückhalt Ettisbühl/Malters (Debris retention at Ettisbühl/Malters). *Wasser Energie Luft* **102**(4), 169–274.

Tsikata, J. M., Katopodis, C. & Tachie, M. F. 2009 Experimental study of turbulent flow near model trashracks. *Journal of Hydraulic Research* **47**(2), 275–280.

Tsikata, J. M., Tachie, M. F. & Katopodis, C. 2014 Open-channel turbulent flow through bar racks. *Journal of Hydraulic Research* **52**(5), 630–643.

Weitbrecht, V. & Rüther, N. 2009 Laboratory and numerical study on sediment transfer processes in an expanding river reach. In: *Proceedings of the 33rd Congress of IAHR*. International Association for Hydraulic Research, Vancouver, Canada, pp. 5436–5443.

Zayed, M., El Molla, A. & Sallah, M. 2018a An experimental investigation of head loss through a triangular 'V-shaped' screen. *Journal of Advanced Research* **10**, 69–76. https://doi.org/10.1016/j.jare.2017.12.005.

Zayed, M., El Molla, A. & Sallah, M. 2018b An experimental study on angled trash screen in open channels. *Alexandria Engineering Journal* **57**(4), 3067–3074. https://doi.org/10.1016/j.aej.2018.05.005.

Zayed, M., El Molla, A. & Sallah, M. 2020 Experimental investigation of curved trash screens. *Journal of Irrigation and Drainage Engineering* **146**(6), 06020003. https://doi.org/10.1061/(ASCE)IR.1943-4774.0001472.